Seismic Laboratory Testing of Energy-Efficient, Staggered-Stud, Wood-Frame Shear Walls

Tonatiuh Rodriguez-Nikl, P.E., M.ASCE[1]; Rakesh Gupta, M.ASCE[2];
Anthonie Kramer, A.M.ASCE[3]; and Arijit Sinha, M.ASCE[4]

Abstract: Residential energy use is a significant contributor to greenhouse gas emissions and climate change. Reducing energy efficiency in conventional wood-framed houses are thermal bridges: direct paths that allow heat to flow through the studs instead of the insulation. One suggestion for reducing thermal bridging is the staggered stud (SS) wall. SS walls use 2×6 bottom and top plates with 2×4 studs alternating between sides of the wall. This allows sheathing to be applied to both sides while eliminating thermal bridges. A literature review has revealed a lack of laboratory test data for SS walls used as shear walls, raising concerns about their safety. The objective of this study was to evaluate the seismic performance of typical SS walls and compare their behavior to similar conventional walls. Monotonic and cyclic laboratory tests were conducted with and without gypsum wallboard. The staggered stud specimens performed similarly to conventional walls. Some minor differences were identified, but the data raised no immediate concerns about the use of SS walls as an energy efficient option in areas of seismic hazard. **DOI: 10.1061/(ASCE)ST.1943-541X.0000894.** *© 2014 American Society of Civil Engineers.*

Author keywords: Energy efficiency; Seismic tests; Shear walls; Wood structures.

Introduction

Energy use in buildings is a significant contributor to greenhouse gas emissions and climate change. The residential sector uses over 20% of the energy in the U.S., attributable in large part to heating (DOE 2010). Improving the energy efficiency of residential construction can play a significant role in addressing these pressing issues. One strategy for improving residential energy efficiency is improving the insulation of the exterior walls. Framing in a typical wood-framed wall creates thermal bridges, i.e., direct paths that allow heat to flow around insulation. In response to this problem, several novel framing patterns have been proposed to break thermal bridges in external walls. One such suggestion is the staggered-stud (SS) wall. SS walls use 2×4 studs with 2×6 bottom and top plates. Studs alternate between sides of the wall (Fig. 1), allowing sheathing to be applied to both sides while eliminating the thermal bridges. Such walls, already used in party walls for sound insulation, can contribute to a more energy-efficient building envelope.

The energy efficiency of building component is often expressed by its R-value, in units of $m^2 \cdot K/W$ ($ft^2 \cdot F \cdot h/Btu$). Heat flow is inversely proportional to the R-value, meaning that components with higher R-values are more efficient. To compute the R-value of a component composed of individual parts connected in series,

the individual R-values are summed. For components in parallel, the reciprocal of the total R-value (called the U-value) is the sum of the individual U-values. Estimates of R-values for different wall types were calculated by using this approach and the following component R-values from Krigger and Dorsi (2009) [$m^2 \cdot K/W$ ($ft^2 \cdot h/Btu$)]: framing, 0.87 per 100 mm (1.25 per in.); R-13 insulation, 2.57 per 100 mm (3.7 per in.); outer air film, 0.030 (0.17); exterior wood siding, 0.143 (0.81); sheathing, 0.141 (0.80); gypsum wall board, 0.079 (0.45); and inner air film, 0.120 (0.68). The results are shown in Table 1. Compared to conventional 2×4 walls, the SS walls provide a 51% to 58% improvement, depending on stud spacing. Compared to conventional 2×6 walls, the SS walls provide a 4% to 9% improvement, depending on stud spacing. These results indicate that SS walls are a suitable choice for improving the energy efficiency of residential wall construction. The previous calculations considered only a clear section of wall away from perimeter framing, yielding an upper limit to energy efficiency. Straube and Smegal (2011) performed detailed energy simulations on various wall types, taking perimeter framing into account. Their results, also presented in Table 1, provide more realistic estimates of full wall efficiency. Extrapolating from their data suggests that the full-wall efficiency of the SS wall is approximately 2.6 $m^2 \cdot K/W$ (15 $ft^2 \cdot F \cdot h/Btu$).

Although there is experience using SS walls as party walls, when used as exterior walls for energy efficiency, SS walls will often be employed as shear walls. This touches on a broader concern about innovative designs that aim to reduce environmental impacts: the potential for inadvertently increasing natural hazard risk in an effort to rush the use of new, untested solutions. Although energy efficiency is an important consideration for sustainability, it is also important to maintain occupant safety [Kestner et al. (2010) provide a full discussion of sustainability as it relates to structural engineering]. FEMA (2010) recognized the link between natural hazards and sustainability in residential construction and specifically identified staggered stud walls as presenting possible concerns under wind or seismic loading. Despite this, the structural building code treats SS walls no differently than conventional walls. Although it may be argued that an SS shear wall is no

[1]Assistant Professor, Dept. of Civil Engineering, California State Univ., 5151 State University Dr., Los Angeles, CA 90032 (corresponding author). E-mail: trodrig7@calstatela.edu

[2]Professor, Wood Science and Engineering, Oregon State Univ., 119 Richardson Hall, Corvallis, OR 97331.

[3]Graduate Student, Wood Science and Engineering, Civil and Construction Engineering, Oregon State Univ., 119 Richardson Hall, Corvallis, OR 97331.

[4]Assistant Professor, Wood Science and Engineering, Oregon State Univ., 119 Richardson Hall, Corvallis, OR 97331.

Fig. 1. The 2×6 bottom plate and 2×4 framing in an SS wall

Table 1. R-Values of Different Wall Types

Wall type (type, stud spacing)	R-value [m² · K/W · (ft² · F · h/Btu)]	
	Clear section of wall	Full wall (Straube and Smegal 2011)
SS, 610 mm (24 in.)	3.84 (21.8)	—
2×6, 610 mm (24 in.)	3.70 (21.0)	—
2×6, 406 mm (16 in.)	3.54 (20.1)	2.48 (14.1)
2×4, 610 mm (24 in.)	2.54 (14.4)	—
2×4, 406 mm (16 in.)	2.43 (13.8)	1.78 (10.1)

different than a conventional wall with plywood on only one side, an extensive review of the literature highlighted a lack of laboratory test data to quantify the seismic behavior of such walls. The objective of this study was to evaluate the seismic performance of typical SS walls and to compare their behavior to similar conventional walls. Monotonic and cyclic laboratory tests were conducted with and without gypsum wallboard (GWB). These tests and the results are described next. Conclusions and limitations appear at the end of the paper.

Materials and Methods

Test Setup and Instrumentation

The test setup and instrumentation are illustrated in Fig. 2. All wall specimens were placed on a steel base and secured by anchor bolts and hold-downs at each end of the wall. The tops of the walls were secured against movement perpendicular to the wall (out-of-plane) by struts located at each corner. Load was applied at the top through a steel beam attached at various points on the top plate. The steel beam was moved in displacement control by a servo-controlled actuator with a capacity of 110 kN (25 kip) and a stroke of ±130 mm (5 in.).

A load cell built into the actuator measured the applied force. The displacement signal from the actuator was used to measure the displacement of the steel beam. The relative displacement between the steel beam and the top plate was measured to allow for the correction of relative motion between the two. At the base of the wall, uplift was measured at each end, as was the slip between the wall and the foundation. The data acquisition system recorded at five
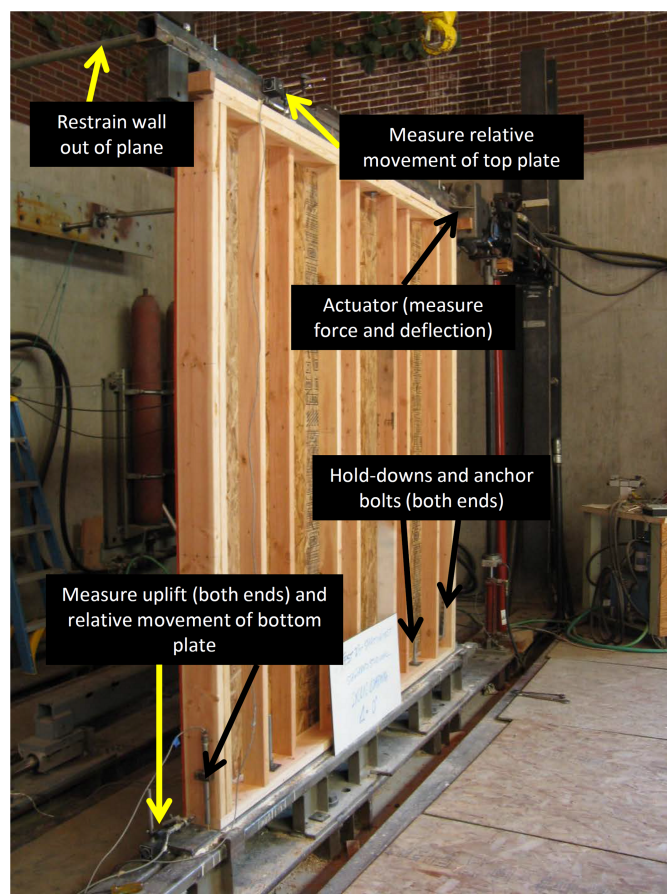

Fig. 2. Test setup and instrumentation

samples per second in monotonic tests and 10 samples per second in cyclic tests.

An optical measurement instrument based on the principles of digital image correlation (DIC) was used to track the out-of-plane displacements of the studs during monotonic tests (DIC displacement measurements were captured at a rate of one sample every 10 seconds). DIC is a full field, noncontact technique for the measurement of displacements and strains (Sutton et al. 1983). The application of DIC for shear wall assemblies has been previously demonstrated successfully by Sinha and Gupta (2009), who provide more background. The setup consisted of a pair of cameras arranged at an angle to take stereoscopic images of the area of interest. Speckled targets were attached to the top plate and select studs. The images were processed by using *Vic-3D*.

Loading Protocols

Monotonic tests were loaded at a constant displacement rate of 6.4 mm/min (0.25 in./min). The walls were pushed to a deflection of 130 mm (5 in.) or beyond, unless a clear failure was observed at a lower deflection, or, as occurred in two tests, the sheathing was observed to impinge on the steel foundation. Distress in the wall was noted in real time and brief stops were made at increments of 13 mm (0.5 in.), if necessary, to photograph interesting behavior. All specimens were photographed before and after the test. The loading protocol was consistent with ASTM E564 (2006).

The cyclic tests were loaded according to ASTM E2126 (2010). The ASTM standard allows for three different cyclic protocols. Test Method 3 (CUREE basic loading protocol) was used for these tests. The loading protocol, shown in Fig. 3, is defined by a reference
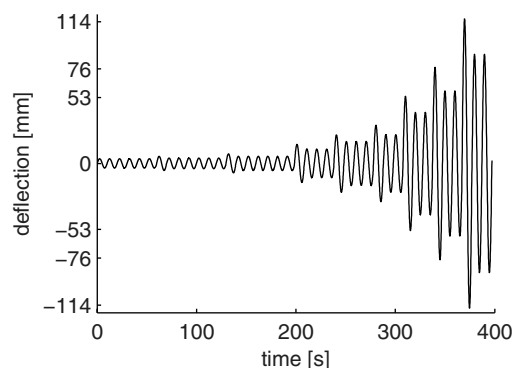
Fig. 3. Loading protocol indicating magnitude of deflection used in the final three cycles

Table 2. Test Matrix

Loading	GWB	Stud configuration	Number of tests
Monotonic	No	C4	2
		C6	2
		SS	2
	Yes	C4	2
		C6	2
		SS	2
Cyclic	No	C6	2
		SS	3
	Yes	C6	2
		SS	2

deflection obtained from monotonic tests. In these tests, a reference deflection of 76.2 mm (3.00 in.) was used. The displacement-controlled loading protocol imposes well-defined loading cycles to the specimen. It begins with six small cycles, then imposes primary cycles at magnitudes of 5, 7.5, 10, 20, 30, 40, 70, 100, and 150% of the reference deflection. Each primary cycle is followed by a specified number of smaller cycles before the next primary cycle is applied. The loading was applied at a rate of 10 s per cycle.

Materials

Walls were built with No. 1, surface dry, Douglas fir lumber from Seneca Sawmill (Eugene, Oregon). Three types of nails were used in construction: 16d nails [89 mm $(3-1/2$ in.$)$ long $\times$ 3.33 mm $(0.131$ in.$)$ diameter, manufactured by Senco (Cincinnati, Ohio)], 10d nails [76 mm $(3$ in.$)$ long $\times$ 3.33 mm $(0.131$ in.$)$ diameter, Huttigrip brand distributed by Huttig (Tigard, OR)], and 8d nails [60 mm $(2-3/8$ in$)$ long $\times$ 2.87 mm $(0.11\,3$ in.$)$ diameter, manufactured by Senco]. Walls were sheathed with oriented strand board (OSB). The OSB was APA 24/16, Exposure 1 rated sheathing with a nominal thickness of 11.1 mm (7/16 in.). GWB measured 13 mm (1/2 in.) in thickness and was attached with 41 mm $(1-5/8$ in.$)$ coarse thread drywall screws. The bottom plate was secured with two 15.9 mm (5/8 in.) anchor bolts with BP 5/8-2 bottom plates by Simpson Strong-Tie (Pleasanton, California). End posts were secured with Simpson Strong-Tie PHD5-SDS3 hold-downs with 15.9 mm (5/8 in.) bolts.

Specimens

The types of specimens tested were selected to compare the behavior of SS walls to that of conventional walls. Both 2×4 and 2×6 conventional walls were tested in the monotonic tests. Because walls with GWB are known to have a higher strength but lower ductility (Van de Lindt 2004), specimens with and without GWB were tested. The resulting test matrix is provided in Table 2. Specimen types were denoted C4 for 2×4 conventional walls, C6 for 2×6 conventional walls, and SS for staggered-stud walls.

All specimens were designed to conform to the *2006 International Residential Code* [International Code Council (ICC 2006)]. Specimen drawings are provided in Figs. 4 and 5. The walls were 2.44×2.44 m $(8 \times 8$ ft$)$ square panels. The frame was built with a single bottom plate, double end posts, a double top plate, and single studs in the interior. All double members were connected with two 10d nails every 610 mm (24 in.). End nailing was with two 16d nails at the top and bottom of each post or stud. OSB panels were attached vertically to the frame with 8d nails at 152 mm (6 in.) on

the edge and 305 mm (12 in.) in the field. As given by the American Wood Council (2007), the shear strength in these walls was 7.0 kN/m (480 lb/ft). This works out to 17.1 kN (3,840 lb) for the 2.44 m (8 ft) wall. When used, GWB was attached horizontally with drywall screws every 305 mm (12 in.) on every available post or stud. The horizontal arrangement was used to eliminate the need for cutting GWB panels to match the staggered stud arrangement. Because the studs were staggered, the SS walls used 33 drywall screws, whereas the conventional walls used 29. This should be kept in mind when interpreting results. All specimens were built in a specially designed fixture that was used to align lumber properly and to minimize differences between test specimens.

Data Analysis Procedures

All load-deflection curves were corrected to remove the effect of relative motion between the loading ram and the top plate of the wall. ASTM E564 (2006) allows for the possibility of using uplift and deflection at the base to correct for rigid body translations and rotations. This correction was not made because the behavior of interest was the as-installed behavior of the wall. Uplift and sliding at the base were recorded to monitor test data for anomalies, but none were observed. Uplift was roughly linear with top plate deflection and did not exceed 11 mm (0.43 in.) in any of the tests. Sliding of the bottom plate did not exceed 3.3 mm (0.13 in.) in any of the tests. In addition to the previously discussed correction, monotonic data were also smoothed lightly to remove noise.

Cyclic load-deflection curves were further processed to find the envelopes (backbone curves) in both directions of loading. Envelopes are often computed by manually picking the peak load and corresponding deflection for each major load cycle. This can result in some of the original data falling outside the envelope. For this paper, a more sophisticated algorithm was employed to find envelopes that wrapped exactly around the data. The cyclic load-deflection curves were also used to compute energy dissipation attributable to hysteresis. This was accomplished by using the trapezoidal rule to integrate the signed area between the curve and the horizontal axis.

As allowed by ASTM E2126 (2010), an average load-deflection curve was computed for each specimen type by averaging the force values at each value of deflection for each specimen type. Minimum and maximum curves were computed in a similar way. For each specimen type, the average, minimum, and maximum curves were calculated up to the smallest of the measured final deflections in each test. Averages for monotonic curves were computed directly from the corrected load-deflection data. Averages
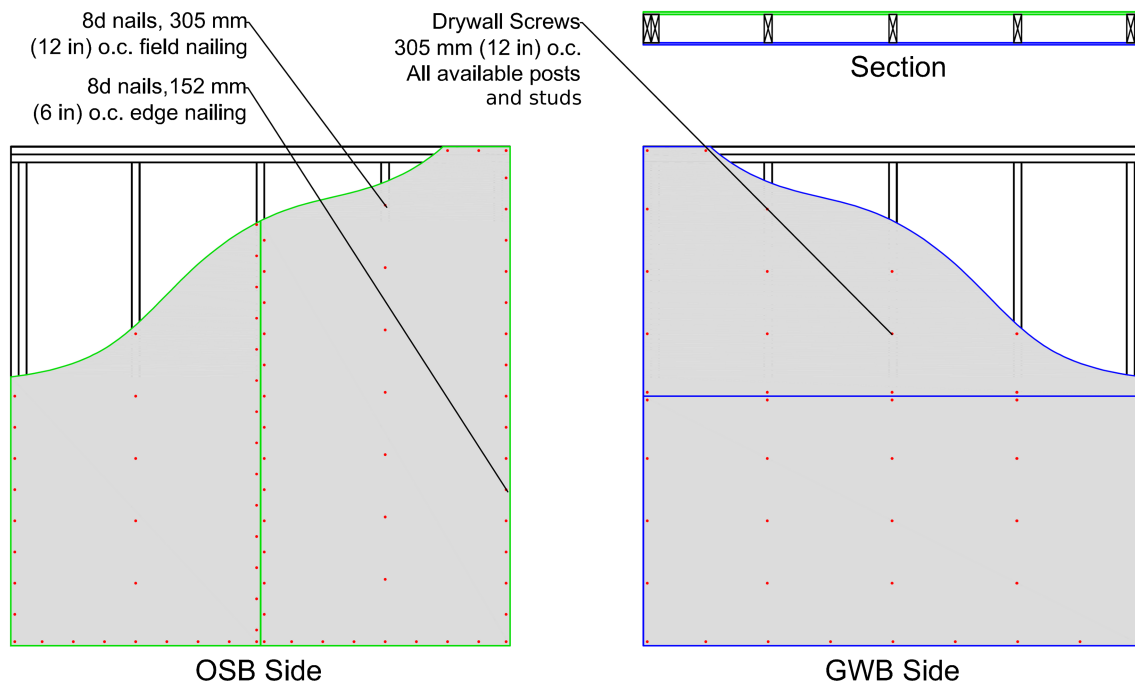
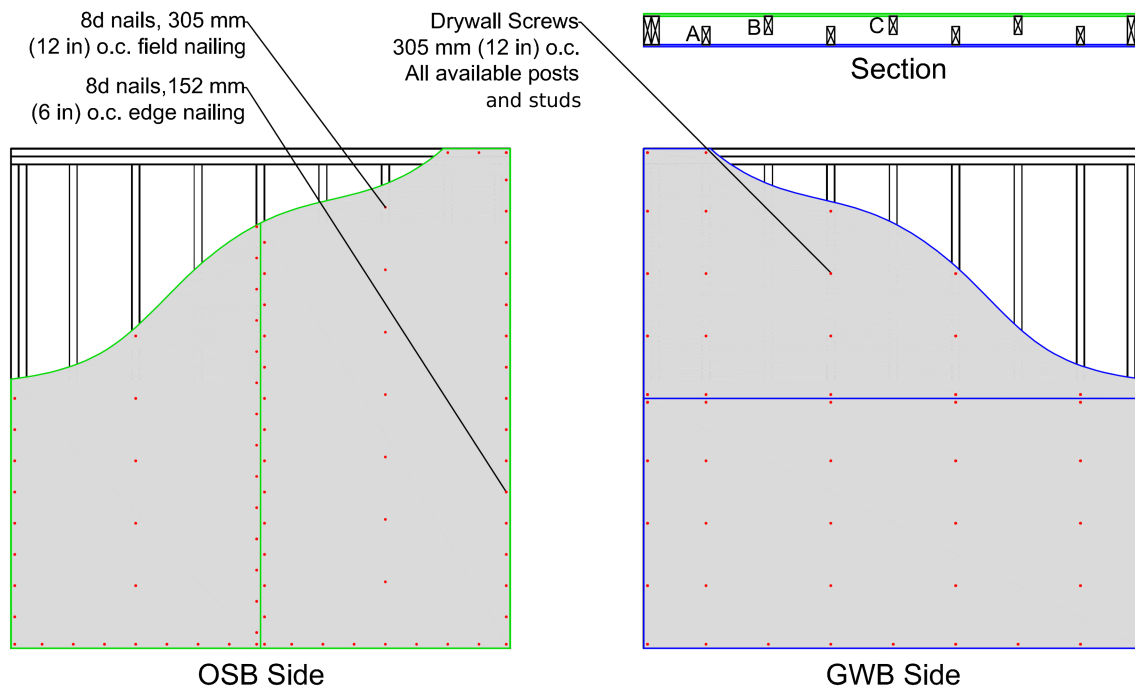**Fig. 4.** Drawing of conventional wall (o.c. = on center)

Fig. 5. Drawing of SS wall (o.c. = on center)

for cyclic tests were computed by using two envelopes for each test.

The average curve for each of the 10 specimen types was used to determine representative parameters. These included load and corresponding deflection at the peak, at 40% of the peak (before reaching peak), and at 80% of the peak (after reaching peak). These are denoted as P_u, Δ_{Pu}, P_{40}, Δ_{P40}, P_{80}, and Δ_{P80}, respectively, and shown in Fig. 6. The deflection Δ_{P80}, which indicates the deflection at which significant load-carrying capacity was lost, is

defined as the ultimate displacement, even in the absence of catastrophic failure. Secant stiffness was computed at each of the load levels by dividing load by deflection. The stiffnesses are denoted as G_u, G_{40}, and G_{80} for Δ_{Pu}, Δ_{P40}, and Δ_{P80}, respectively. Finally, the equivalent energy elastic-plastic (EEEP) curve was computed as defined by ASTM E2126 (2010). The EEEP curve is defined by the points (0,0), (Δ_y, P_y), and (Δ_{P80}, P_y). The yield load P_y is computed so that the area underneath the EEEP curve was the same as the area under the recorded curve (ignoring data beyond Δ_{P80}).
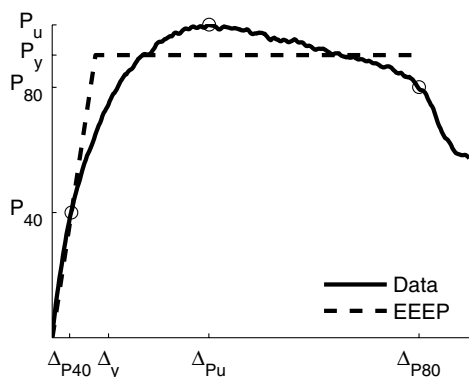
Fig. 6. Representative parameters shown on an average load-deflection curve and the corresponding EEEP curve

The EEEP curve is forced to go through the point (Δ_{P40}, P_{40}) by defining the deflection Δ_y as P_y/G_{40}. The EEEP curve is used to provide an idea of ductility through a ductility ratio $D = \Delta_{P80}/\Delta_y$. The EEEP curve is also shown in Fig. 6.

For each DIC target, only the out-of-plane component was used. Because the targets protruded from the specimen, vertical and longitudinal deflection were prone to error as a result of rotation. Despite this, the horizontal deflections measured in the top plate were very close to the actuator deflection, which provides confidence in the DIC data. For each stud that was instrumented, the out-of-plane deflection at midheight was used directly as recorded.

Results and Discussion

Overall results are provided in Fig. 7, which displays shaded areas defined by the minimum and maximum curves for each specimen type; Table 3, which details the observed failure modes for each test; and Table 4, which lists the representative parameters computed for each specimen type. Results are discussed next in the following order: monotonic tests without GWB, monotonic tests with GWB, out-of-plane motion in monotonic tests, and cyclic tests. A summary is provided at the end.

Monotonic Tests without GWB

The load-deflection plots [Fig. 7(a)] and the ultimate values in Table 4 indicate that the strength of the C4 specimens was greater, followed by the C6, and the SS. The shaded areas overlapped for all specimens, indicating that differences between specimens were minor. Ultimate strength was lower than the code value for all three specimens. At low deflections, a large stiffness was recorded for the C6 specimens. The different specimen types differed significantly in terms of ultimate displacement. This is shown both in Fig. 7(a) and in the 80% postpeak values in Table 4. In SS walls, failure occurred as early as 75 mm (3 in.) of displacement; in C4 specimens, approximately 100 mm (4 in.); and in C6 specimens, nearly at 130 mm (5 in.). In the latter case, 20% of the strength was lost by approximately 100 mm (4 in.) of displacement. In all cases, the same two distinct failure modes were observed for each specimen type. One failure mode consisted of the separation of framing members, which led to excessive loading in the sheathing nails and a rapid failure. The other failure mode was a more gradual process of bending and pullout of the sheathing nails. Both failure modes are shown in Fig. 8. The variability of deflection at which the separation of framing occurred was responsible for the variability in failure deflection. The EEEP values in Table 4 indicate that the ductility factor of the C6 specimens was greater than the other two types, but in this case, the ductility factor was less representative of a large ultimate deflection and more of large initial stiffness.
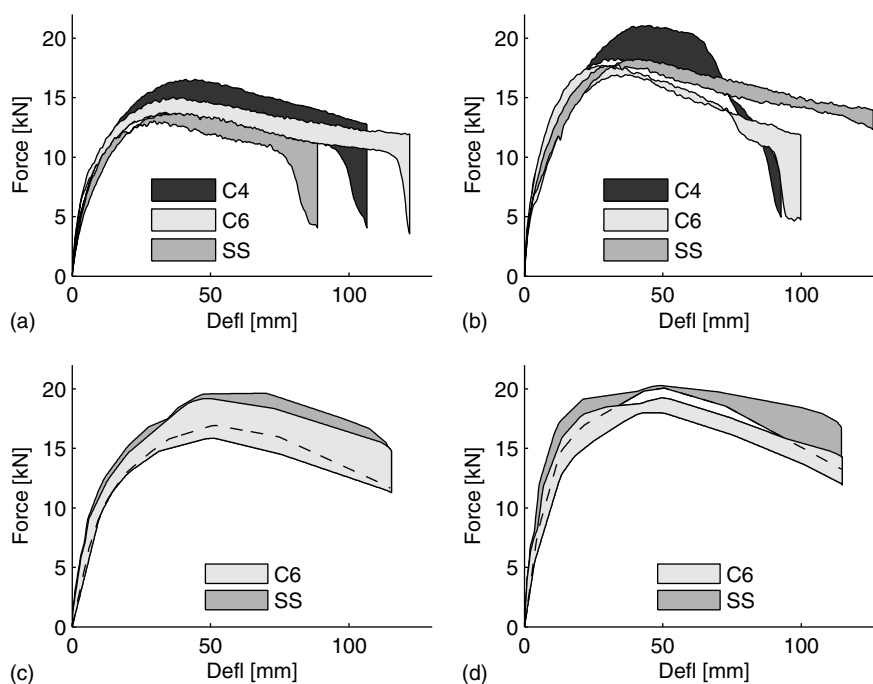

Fig. 7. Bounds of test results for each test type (plotted up to the smallest of the final deflections for each type): (a) monotonic without GWB; (b) monotonic with GWB; (c) cyclic without GWB; (d) cyclic with GWB

Table 3. Observed Failure Modes

Loading	GWB	Stud config.	Failure mode
Monotonic	No	C4 C6 SS	All three specimen types exhibited the same two distinct failure modes: 1. No catastrophic failure, nail pullout, or bending 2. Separation of top plate from studs, leading to pullout and bending of nails (some tear-through)
	Yes	C4	Separation of top plate from studs, leading to pullout and bending of nails (some tear-through)
		C6	Both specimen types exhibited the same two distinct failure modes: 1. No catastrophic failure, nail pullout, or bending
		SS	2. Separation of top plate from studs, leading to pullout and bending of nails (some tear-through)
Cyclic	No	C6 SS	No catastrophic failure; nail pullout and bending (some tear-through); some stud separation observed in approximately half of the specimens
	Yes	C6 SS	

Note: All tests with GWB experienced fracture of drywall screws and some tearing of GWB.

Monotonic Tests with GWB

The load-deflection plots [Fig. 7(b)] illustrate that the C6 and SS specimens had similar peak behavior, but that at the peak, the C4 specimens varied significantly [the difference in strength between C4 tests was less than 15%, which is within the acceptable limits of ASTM E564 (2006)]. At lower deflections, all specimens had similar stiffness of between 1.8 kN/mm (10 kip/in.) and 1.9 kN/mm (11 kip/in.). Both types of conventional walls failed between 75 (3 in.) and 100 mm (4 in.), whereas the SS wall did not experience catastrophic failure. Because of this, the EEEP values indicate a higher ductility factor for the SS walls. Similar failure modes were observed in the OSB for these walls, as in the test without GWB. The postpeak slope of the SS specimens was noticeably less steep than the other specimen types, indicating that the SS walls maintained strength better at large deflections. Comparing differences between specimens with and without GWB (Fig. 9), the conventional walls followed the expected pattern of higher

strength and lower ductility when GWB is added. The SS walls, although exhibiting the expected increase in strength, also exhibited large increases in ductility.

Out-of-Plane Motion in Monotonic Tests

The out-of-plane deflection prior to failure was less than 8 mm (0.3 in.) in all tests but one, which experienced deflections up to 13 mm (0.5 in.). Nearing failure, studs in several of the tests suffered larger deflections attributable to lack of lateral restraint once framing members separated. As shown in Fig. 8, this allowed the OSB to pull the stud laterally as the bottom row of sheathing nails failed, forcing the OSB and the stud away from the wall. The recordings of out-of-plane deflection demonstrated decoupling between both sides of the SS walls. A typical example is shown in Fig. 10. Very small deflections were recorded during the ascending part of the load-deflection curve. During the descending branch (postpeak), deflection in the two studs attached to the OSB changed suddenly. As each of the studs separated from the bottom plate, and as the failure in the sheathing nails progressed toward the center of the wall, each of the studs pulled away from the wall, in one case up to 15 mm (0.6 in.). In contrast, the stud connected to the GWB remained relatively steady, deflecting less than 2 mm (0.1 in.). Although the studs attached to the GWB were not pulled laterally as a result of failure of studs on the other side, they were also unable to provide restraint that might have mitigated the effects of failure. Despite these results, the deflections of the studs were not associated with any sudden change in capacity, suggesting that the differences, although interesting, are not of practical importance. Further investigation is necessary to determine whether out-of-plane deflections might indicate greater susceptibility to buckling of the partially supported studs in the presence of gravity loads.

Cyclic Tests

There was significant overlap in the load-deflection envelopes [Figs. 7(c and d)], especially for the tests without GWB. In both cases, as indicated by both the plots and the ultimate values, the ultimate strength of the SS walls was slightly larger. The ultimate strength of all specimens exceeded code capacity. At smaller deflections, the stiffness of the SS walls was also higher. No catastrophic failure occurred in any of the cyclically loaded walls. All specimen types reached 80% of peak strength at approximately 100 mm (4 in.) of displacement. Ductility factors were all between 8 and 9, except for SS walls with GWB, which had a larger

Table 4. Representative Parameters for Each Test Type

Loading	GWB	Stud config.	40% Pre-peak			Ultimate			80% Post-peak			EEEP		
			$P40$ (kN)	$\Delta P40$ (mm)	$G40$ (kN/mm)	P_u (kN)	Δ_{Pu} (mm)	$G100$ (kN/mm)	P_{80} (kN)	Δ_{P80} (mm)	G_{80} (kN/mm)	P_y (kN)	Δ_y (mm)	D
Monotonic	No	C4	6.08	4.1	1.50	15.2	45	0.34	12.2	94	0.13	13.7	9.1	10.3
		C6	5.74	2.8	2.05	14.3	33	0.43	11.5	104	0.11	12.7	6.2	16.8
		SS	5.31	4.1	1.31	13.3	33	0.40	10.6	78	0.14	12.0	9.2	8.5
	Yes	C4	7.82	4.1	1.92	19.5	39	0.50	15.6	73	0.22	17.6	9.1	8.0
		C6	6.88	3.6	1.94	17.2	31	0.55	13.8	74	0.19	15.4	8.0	9.3
		SS	7.15	4.1	1.76	17.9	37	0.48	14.3	105	0.14	15.9	9.0	11.6
Cyclic	No	C6	6.89	5.6	1.23	17.2	50	0.34	13.8	106	0.13	15.4	12.5	8.5
		SS	7.24	5.6	1.30	18.1	51	0.36	14.5	103	0.14	16.2	12.5	8.3
	Yes	C6	7.43	4.8	1.54	18.6	50	0.38	14.9	97	0.15	16.9	10.9	8.9
		SS	8.05	4.3	1.86	20.1	50	0.40	16.1	107	0.15	18.2	9.8	10.9

Fig. 8. Two failure modes were observed: pullout and bending of sheathing nails (occasional pull-through) and separation of framing members
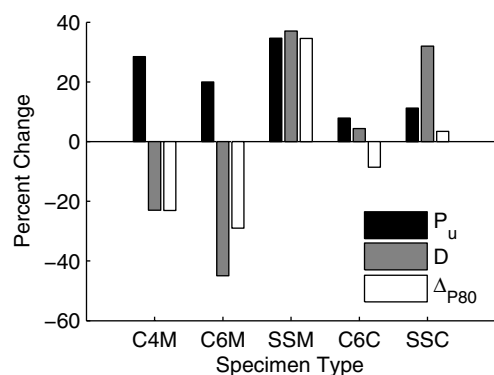

Fig. 9. Differences between tests with and without GWB (C = cyclic; M = monotonic)

Fig. 10. Example of out-of-plane motion of the studs, shown with corresponding load-deflection curve (stud labels refer to Fig. 5)

Fig. 11. Upper and lower bounds of cumulative hysteretic energy (last 20 cycles of cyclic tests)

ductility factor. This is mostly attributable to the larger value of Δ_{P80} in these tests, and to a lesser extent, the larger initial stiffness. Consistent with observations in the monotonic tests, the SS walls in the cyclic tests also exhibited an increase in ductility when GWB was added (Fig. 9). Energy dissipation (Fig. 11) was the same in the SS and C6 walls without GWB. Walls with GWB dissipated more hysteretic energy, but the SS walls dissipated much more, potentially because of the greater number of drywall screws.

Summary of Relevant Results

Compared to conventional walls, monotonically loaded SS walls had lower ductility and a smaller failure deflection. Although the ductility of conventional walls decreased when GWB was added, it increased for SS walls. In monotonic tests with GWB, SS walls lost strength more slowly than conventional walls. In cyclic tests, SS walls with GWB dissipated more hysteretic energy than conventional walls. Out-of-plane measurements indicated that the two sides of SS walls were decoupled, but this was not linked to any noticeable change in the load-deflection curve.
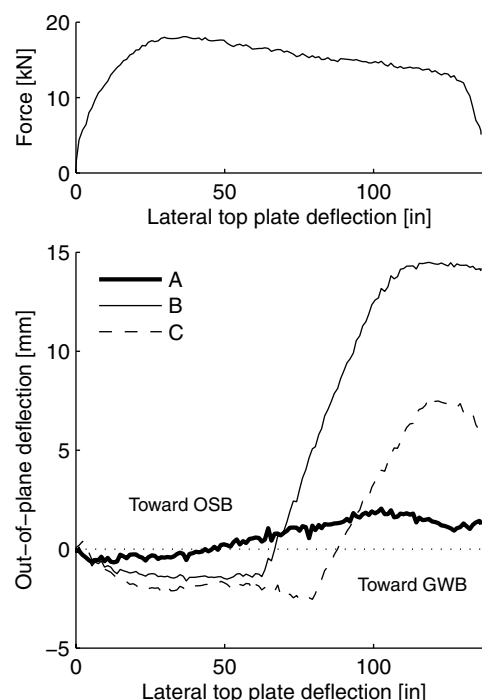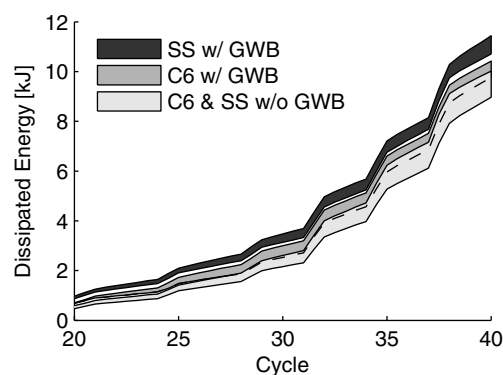
Conclusions

This study compared the performance of SS and conventionally framed walls, using typical details for residential construction. The fundamental conclusion is that, for the nail spacing, nail type, and sheathing used, there is no significant reason to reject SS walls on the basis of seismic performance. Although some differences were observed in the behavior of SS and conventional walls, none of these differences presented significant concerns or benefits. Care should be taken not to extend the results to nail spacing, nail type, sheathing type, or sheathing arrangements that were not tested, nor should results be extended to walls with large gravity loads. Additional testing may be necessary to establish conclusively the safety of SS walls. Within these constraints, given the similarity in performance, adequate strength and ductility, and improved energy efficiency of up to 58% compared with conventional walls, there is good reason to consider the use of SS walls in residential

construction. The benefits in the energy efficiency of SS walls must be weighed against the potential difficulty of construction and increased material use. In addition, the use of SS walls should be viewed in conjunction with other energy-saving strategies such as air sealing, energy-efficient windows, and appropriately sized mechanical systems (APA 2008). Beyond the SS walls tested in this study, efforts to improve residential energy efficiency should include continued attempts at innovation in wood framing, e.g., fitting rigid foam insulation between the framing and structural sheathing (APA 1999), or revival of older framing techniques, e.g., diagonal bracing of walls with rigid insulation (Fisette 1993). No matter the proposed system, researchers, engineers, code officials, and builders are encouraged to consider carefully the disaster resilience of structural systems when trying to reduce the impacts of buildings on the environment.

Acknowledgments

References

American Wood Council. (2007). *Special design provisions for wind and seismic with commentary*, 2005 Ed., American Forest and Paper Association American Wood Council, Washington, DC.

APA—The Engineered Wood Association. (1999). "APA rated siding panels over rigid foam insulating sheathing." *Technical Note C465D*, APA, Tacoma, WA.

APA—The Engineered Wood Association. (2008). "Build energy efficient walls." *Form No. J440*, APA, Tacoma, WA.

ASTM. (2006). "Standard practice for static load test for shear resistance of framed walls for buildings." *E564-06*, West Conshohocken, PA.

ASTM. (2010). "Standard test methods for cyclic (reversed) load test for shear resistance of vertical elements of the lateral force resisting systems for buildings." *E2126-10*, West Conshohocken, PA.

DOE. (2010). *Annual energy review 2010*, 〈http://www.eia.gov/total energy/data/annual/pdf/sec2_4.pdf〉 (Aug. 16, 2012).

FEMA. (2010). "Natural hazards and sustainability for residential buildings." *FEMA P-798*, Washington, DC.

Fisette, P. (1993). "Bracing foam-sheathed walls." *J. Light Constr.*

International Code Council (ICC). (2006). *International residential code for one- and two-family dwellings*, ICC, Washington, DC.

Kestner, D. M., Goupil, J., and Lorenz, E., eds., (2010). *Sustainability guidelines for the structural engineer*, ASCE, Reston, VA.

Krigger, J., and Dorsi, C. (2009). *Residential energy: Cost savings and comfort for existing buildings*, 5th Ed., Saturn Resource Management, Helena, MT.

Sinha, A., and Gupta, R. (2009). "Strain distribution in OSB and GWB in wood-frame shear walls." *J. Struct. Eng.*, 10.1061/(ASCE)0733-9445 (2009)135:6(666), 666–675.

Sutton, M. A., Wolters, W. J., Peters, W. H., Rawson, W. F., and McNeill, S. R. (1983). "Determination of displacements using an improved digital image correlation method." *Image Vis. Comput.*, 1(3), 133–139.

Straube, J., and Smegal, J. (2011). *Building America special research project: High-R walls case study analysis*, Building Science, Somerville, MA.

Van de Lindt, J. W. (2004). "Evolution of wood shear wall testing, modeling, and reliability analysis: Bibliography." *Pract. Period. Struct. Des. Constr.*, 10.1061/(ASCE)1084-0680(2004)9:1(44), 44–53.

Vic-3D [Computer software]. Correlated Solutions, Columbia, SC.